

Evaluation of the Parameters Affecting the Photoelectrocatalytic Reduction of CO₂ to CH₃OH at Cu/Cu₂O Electrode

Juliana Ferreira de Brito, Alexander Alves da Silva, Alberto José Cavaleiro and Maria Valnice Boldrin Zanoni*

Institute of Chemistry-Araraquara, UNESP, Rua Francisco Degni, 55 - Bairro Quitandinha, 14800-900, Araraquara - SP - Brazil.

*E-mail: boldrinv@iq.unesp.br

Received: 1 May 2014 / Accepted: 24 July 2014 / Published: 25 August 2014

This work describes the photoelectrocatalytic reducing CO₂ dissolved in slightly alkaline solution at Cu/Cu₂O electrode prepared by electrochemical deposition of a copper foil in 12.0 mol L⁻¹ submitted to voltage of -0.40 V for 30 min. The effect of supporting electrolyte was investigated and 80 ppm of methanol was generated when photoelectrolysis were performed at Cu/Cu₂O electrode in 0.1 mol L⁻¹ Na₂CO₃/NaHCO₃. However, this value is limited to 10 ppm in Na₂CO₃ and is almost neglected in NaHCO₃. The bias potential also plays an important role in the formation of methanol by photoelectrocatalysis, where is maxima at applied potential of 0.2V and nil at -0.4V. Maximum photoconversion of CO₂/CH₃OH was obtained at pH 8, which is successively suppressed in an alkaline medium. Thus, using the best experimental conditions of 0.1 mol L⁻¹ Na₂CO₃/NaHCO₃, pH 8, were obtained 75 % reduction of CO₂ to methanol under UV-Vis irradiation and bias potential of +0.2 V vs Ag/AgCl, after 2 hours of treatment. The results illustrate that the stabilization of Cu (I) on the electrodic material seems to be the key to success in this photoelectrochemical reaction.

Keywords: Cu/Cu₂O semiconductor, CO₂ reduction, methanol, photoelectrocatalytic reduction, carbon dioxide conversion to methanol.

1. INTRODUCTION

Fast-growing carbon dioxide emission and its consequences for the Earth's climate constitute an environmental threat and there is a rapid converging agreement that CO₂ emissions need to be reduced [1-3]. In response to this great challenge, there is a permanent search for efficient way to prevent the accumulation of CO₂, using removal, sequestration and conversion methods able to generate other compounds. Therefore, the development of methods able to recycle CO₂ into value added products and/or through high-energy content fuel has received great attention [4-6].

The conversion and recycling of CO₂ to functional hydrocarbons are persuaded since the early of 1990s and several methods are described in literature, as the use of biomass [6,7], thermochemical [8,9], electrochemical [5,10-16] and photocatalytic processes [17-20]. Among them, electrochemical methods has demonstrated to be a good strategy to reduce CO₂ following the equation: CO_{2(aq)} + e⁻ → CO₂^{•-}. This process is advantageous because it produces oxygenated hydrocarbons with high energetic content [19]. However, there is a large consensus that the electrode reaction and products generated are strongly dependent of pH, CO₂ concentration, nature of the supporting electrolyte, catalyst and mainly of the electrocatalytic activity of the electrode material [10].

In aqueous media, the formation of carbon monoxide by electroreduction of CO₂ is particularly expected at Au, Ag, Zn, Pd and Ga, for instance, while formic acid is generated during reduction at Pb, Hg, In, Sn, Bi, Cd and Tl materials. Some metals such as, Ti, Nb, Ta, Mo, Mn and Al heavily favor hydrogen evolution and electroreduction in nonaqueous medium usually leads to generation of oxalic acid, tartaric acid and glyoxylic acid, for example [19].

Copper and/or copper oxides electrodes have shown great success in the reduction of CO₂. Terumura et al. [14] described the hydrocarbons production of gaseous products, such as hydrogen (H₂), carbon monoxide (CO), methane (CH₄), and ethane (C₂H₄) on copper electrode. Ohya et al. [5] assessed the generation of H₂, CO, and formic acid for electrolysis conducted for CuO and Cu₂O electrodes supported on zinc powder and a methanolic KOH solution. Kuhl et al. [15] employed a metallic copper electrode to reduce CO₂ and studied the 16 products by NMR (Nuclear Magnetic Resonance). However, copper-based electrodes also offer limitations: (1) CO₂ reduction occurs at high potential, so hydrogen evolution competes with the target reaction; and (2) some products arise at the electrode preventing the selective synthesis of a specific product.

The use of photocatalysis process has being also explored as a new method able to photoconvert CO₂ into CO, O₂ and hydrocarbons by using TiO₂ doped with N, Pt, and Cu [14,20,21]. Copper oxide exists as a compound semiconductor in two different metal oxidation states, Cu₂O and CuO, these two compounds have energy band-gaps of 2.0 – 2.2 eV and 1.3 – 1.6 eV, respectively [21,22]. Electrons are transferred from valence band to the conduction band when activated by absorption irradiation, which can be trapped by CO₂ or water [21]. The water and CO₂ reduction compete in the photocatalytic system, since these reactions take place on the photocatalyst/cocatalyst surface simultaneously. Then, specific studies are necessary to improve process efficiency.

An alternative to improve photocatalytic process efficiency is the photoelectrocatalytic, where the photogenerated electrons can be effectively extracted to the outer circuit by applying a potential bias across the semiconductor film, which results in the improved separation of photogenerated electron-hole pairs. Here, the potential gradient applied simultaneously to the light activation determines the photoelectrocatalytic efficiency [21,23]. The literature [24-27] reports the use of p-type semiconductors such as GaP, GaAs, ZnS, CdS, SiC, and WO₃ to reduce photoelectrochemically the CO₂. However, few researches have demonstrated the potentiality of copper electrodes applied in photoelectrochemical conversion of CO₂. Ghadimkhani and co-workers [22] have demonstrated that solar photoelectrosynthesis of methanol was driven on hybrid CuO–Cu₂O semiconductor nanorod arrays with a faradaic efficiencies up to 95% by using sodium sulfate as electrolyte and visible irradiation.

In this paper, we report the photoelectrochemical conversion of dissolved CO₂ in carbonate electrolytes at Cu/Cu₂O electrodes prepared by electrochemical deposition. It was found that the present photocathode displayed a remarkably improved CO₂ reduction activity and parameters like electrolyte, pH and applied potential interferes markedly in the generation of methanol and ethanol. The electrode was activated by commercial lamp irradiating at UV and visible light.

2. EXPERIMENTAL

2.1 Electrochemical preparation of the Cu/Cu₂O Electrode

The Cu/Cu₂O electrodes measuring 1 cm x 1 cm were prepared by electrochemical method [28,29]. A three-electrode electrochemical cell arrangement was used (working electrode = copper foil, counter electrode = platinum foil measuring 1 cm × 1 cm, and reference electrode = Ag/AgCl, KCl_(sat)), operating at 60 °C. The pH of solution was adjusted to 12.0 with 12.0 mol L⁻¹ NaOH based in Sower and Fillinger [30]. A voltage of -0.40 V was applied for 30 min by means of a Potentiostat/Galvanostat AUTOLAB model PGSTAT 302, washed with distilled water and dried with nitrogen. The electrode was used in the photoelectrochemical experiments.

2.2. Characterization of the Cu/Cu₂O Electrode

The X-ray diffraction of the Cu/Cu₂O electrode was recorded on a diffractometer Siemens model D 5000 using radiation in the 4-70° range. The structures and morphologies were characterized by Field Emission Gun Scanning Electron Microscopy (FEG-SEM) conducted on a Zeiss model Supra 35, coupled to an Energy Dispersive X-ray (EDX). Linear voltammetry was carried out at a scan rate of 0.01 V s⁻¹, in the presence and absence of UV radiation, for 0.1 mol L⁻¹ sodium carbonate/bicarbonate buffer solution, 0.1 mol L⁻¹ sodium carbonate solution and 0.1 mol L⁻¹ sodium bicarbonate solution as supporting electrolyte.

2.3 Apparatus and procedure

The photoelectrochemical (PEC) experiments were performed in a 250 mL cylindrical one-compartment glass reactor with cooling system, where the Cu/Cu₂O working electrode was irradiated with UV-Vis light (125-W high pressure mercury lamp from Oriel) vertically inserted in a central quartz bulb. A saturated Ag/AgCl (KCl sat) electrode was used as reference, and the counter electrode consisted of a Pt gauze.

The CO₂ reduction was accomplished under controlled-potential electrolysis and UV-Vis irradiation. The reaction was carried out in 150 mL of supporting electrolyte containing dissolved carbon dioxide by bubbling CO₂ gas (OXI-MEDIN). The quantification of carbon dioxide dissolved was monitored by dissolved inorganic carbon using a total organic carbon analyzer Shimadzu model TOC-V_{CPN}.

2.4. Analysis of the products generated after CO₂ photoelectroreduction

Methanol and ethanol generated as probable product from CO₂ photoreduction were detected and quantified by gas chromatography (GC-FID model CP-3800 Varian) using a solid-phase microextraction technique (SPME). The SPME technique relies on the use of a fiber covered with a thin-selective layer that extracts organic compounds directly from aqueous samples to gas chromatography analysis. For this purpose, a 0.5 mL aliquot of the photoelectrolyzed solution was transferred to a properly closed container (1.5 mL), and subjected to heating in a bath IKA brand model HB 0.5 0.6 CN for 7 min. Then, the fiber was exposed to the vapors for 5 min. After adsorption, the fiber was collected and injected into the gas chromatograph. The chromatographic column consisted of a 30-m long Stabilvax RESTEC column with 0.25-mm internal diameter and 25- μ m film thickness. The carrier gas was nitrogen at a flow rate of 1.0 mL min⁻¹. The injector and detector were maintained at 250 °C. The describing of the heating ramp is 35 °C for 4 min, heating to 45 °C by 1 °C min⁻¹, heating to 120°C by 20°C min⁻¹, and, finally, it was kept in 120 °C for 4.5 min.

Analytical curves of methanol and ethanol were constructed from 0.5 to 40 ppm using the same analytical system; good linearity was achieved in both cases. The correlation coefficient and detection limits were 0.97517, 1.75 μ g L⁻¹ and 0.99307, 2.24 μ g L⁻¹ for methanol and ethanol, respectively.

2.5. Analysis of free copper ion by anodic stripping voltammetry

Tests to monitor the possible copper lixiviation were carried out using anodic stripping voltammetry. The analysis was conducted in a one-compartment electrochemistry cell of three electrodes, glassy carbon electrode as work, platinum foil as counter electrode and Ag/AgCl electrode as reference. In this system was added 50 mL of 1.0 mol L⁻¹ potassium nitrate solution and 40 μ L of solution after the photoelectrochemistry reduction that wanted analyze. This solution is submitted to deaeration with nitrogen gas during 10 min. The potential of -0.7 V was applied in the glassy carbon electrode with magnetic agitation during 5 min. After this process, the anodic stripping voltammetry was realized between -0.20 and 0.15 V with scan rate of 5 mVs⁻¹ [31].

Analytical curve of copper in solution was constructed from 0.03 to 1.70 mg L⁻¹ using the same analytical system; good linearity was achieved. The correlation coefficient and detection limit were 0.996 and 0.10 mg L⁻¹, respectively.

3. RESULTS AND DISCUSSION

3.1 Characteristics of the Photocathode

Figure 1a illustrates the top view SEM micrographs obtained from FEG-SEM image of the Cu/Cu₂O electrode prepared by electrochemical copper oxide deposition. The surface has a well-defined structure and contains pyramid crystals with height ranges between 3 μ m to 400 nm. These crystals refer to copper oxide (I), as reported in the literature [32] and verified by XRD (Figure 1b).

The diffraction peaks at about $2\theta = 43, 45,$ and 50° correspond to metallic copper; the peak at 36° is related to copper oxide (I). The energy dispersive spectroscopy X-ray (EDX) analysis confirms the presence of the elements, which primarily constitute the Cu/Cu₂O electrode – the spectrum displays peaks with relative intensity, typical of the presence of oxygen (0.42 keV) and copper (0.14, 0.7, and 11.4 keV) on the surface.

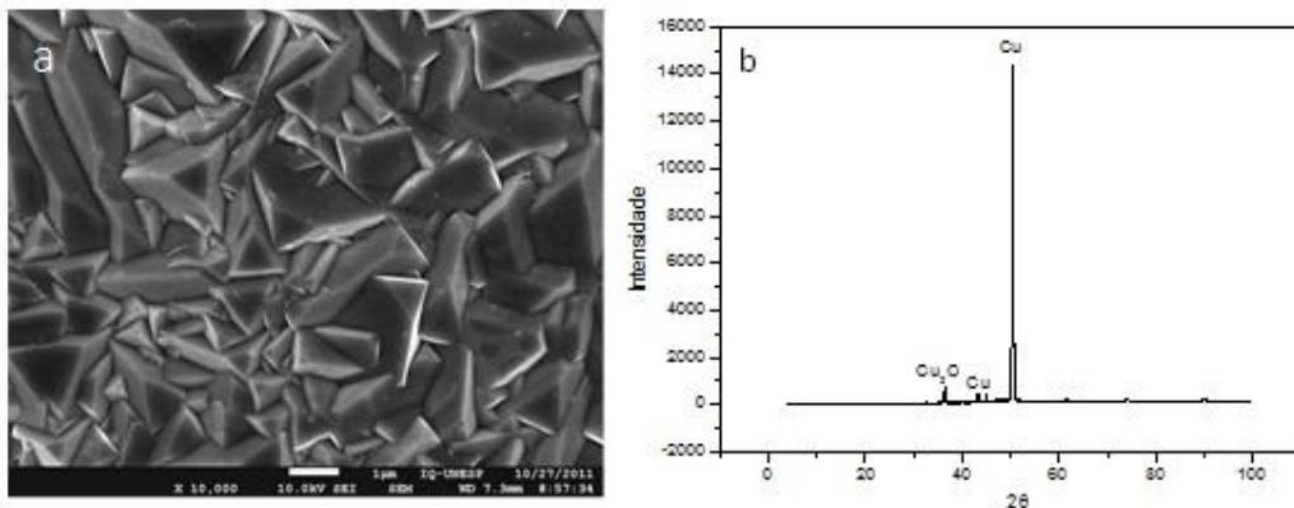


Figure 1. a) FEG-SEM images b) XRD images using radiation in the 4° a 70° range, obtained for Cu/Cu₂O electrode prepared by cathodic deposition in cupric sulfate the 0.4 mol L⁻¹ solution containing sodium lactate 3.0 mol L⁻¹ at pH 12.0, during 30 minutes, temperature = 60 °C and potential = -0.4V.

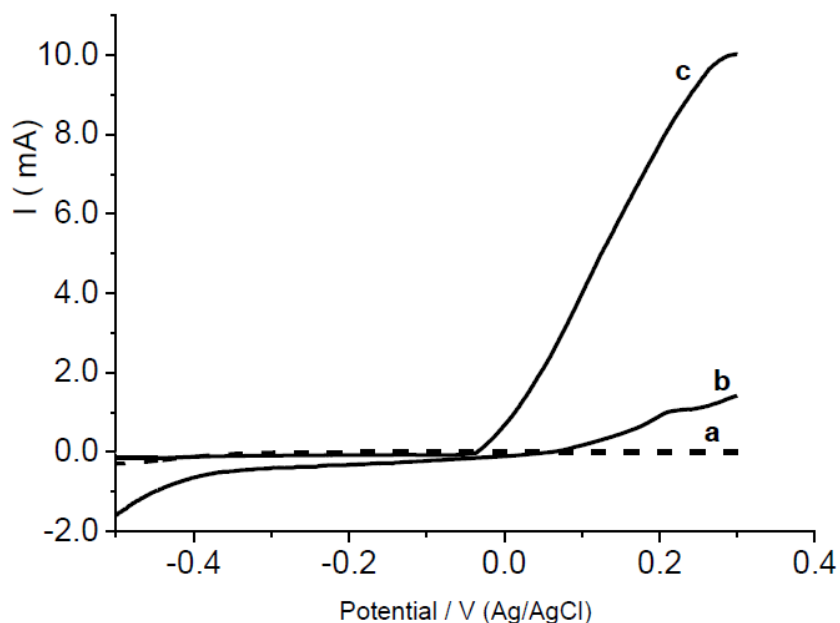


Figure 2. Linear scan voltamograms obtained for Cu/Cu₂O electrode in 0.1 mol L⁻¹ sodium sulfate in the dark (a) and irradiated by UV-Vis light in the absence (b) and presence of 3.3×10^{-3} mol L⁻¹ dissolved CO₂ (c). Scan rate = 10 mV s⁻¹.

Figure 2 shows linear scan voltammograms recorded at 10 mV s^{-1} for Cu/Cu₂O electrode in $0.1 \text{ mol L}^{-1} \text{ Na}_2\text{SO}_4$ under dark (Curve a), irradiated with UV-Vis light (curve b) and dissolved 200 ppm of CO_2 (curve c) at 10 mV s^{-1} . When the electrode surface is photoactivated is possible to see the occurrence of a wave that start at $+0.1 \text{ V}$ and reach a maximum value around $+0.30 \text{ V}$ (curve b), showing the formation of electrons on the conduction band and lacunas in the valence band. These lacunas are able to promote the oxidation of $\text{Cu}^{\text{(I)}}\text{O} \rightarrow \text{Cu}^{\text{(II)}}\text{O} + \text{e}^-$ and or to the bias potential on the electrode surface[33]. Concomitantly, at negative potential higher than -0.4 V is obtained the water reduction forming hydrogen [30]. On the other hand, in the presence of saturated electrolyte of sodium sulfate with CO_2 under UV-Vis irradiation, the respective photocurrent ascend at potential more positive than -0.05 V and the peak taken at $+0.30 \text{ V}$ wave is approximately 10 times higher when CO_2 reduction is taken place. In agreement with literature [33] under photoelectrocatalysis condition the photo-excited holes generated could be trapped by Cu (I) forming Cu (II). The electrons on the conduction band (e^-) could be trapped by adsorbed CO_2 to $\text{CO}_2^{\bullet\text{-}}_{\text{ads}}$ and the Cu (II) species could be also reduced again to Cu (I) species with electron generated in the conduction band under light. Thus, there are a sequential cycle on the surface of Cu₂O, where the electron-hole recombination is minimized and therefore it is observed a marked increase in the photocurrent (Figure 2c) when compared with the photocurrent in the absence of CO_2 (Figure 2b). It is interesting to consider the Cu (I) stability relative to photoelectrochemical condition.

Therefore, using the light and a positive potential of $+0.2 \text{ V}$ the oxidation of Cu^+ to Cu^{2+} is induced, as well as the CO_2 reduction due electrons generated in the system by UV irradiation, yielding a redox cycle of $\text{Cu}^{2+}/\text{Cu}^+$ system in the photoelectroreduction. In addition, it is known that the Cu^+ species could favor the main adsorption sites of CO_2 for methanol production [34]. This affirmation will be confirmed with the assistance of CO_2 reduction experiments and analysis of methanol and ethanol production.

3.2 CO_2 photoelectrochemical reduction

In order to study the reduction of CO_2 by photoelectrocatalysis at Cu/Cu₂O electrode experiments were carried out during 3 h for approximately 200 ppm of CO_2 dissolved in $0.3 \text{ mol L}^{-1} \text{ Na}_2\text{CO}_3$ pH 9 under bias potential of $+0.2 \text{ V}$ and UV-Vis irradiation (Figure 3a). The CO_2 removal percentage increases linearly up to 120 min of photoelectrolysis, reaching a maximum conversion of 80% of CO_2 .

Figure 3b exhibits the current vs time curves recorded during the above photoelectrolysis. The current increase in the first 60 min of electrolysis and decreases thereafter, reaching minimum values after 120 min. This behavior suggests the formation of intermediate $\text{CO}_2^{\bullet\text{-}}$ generated in the beginning of the electrolysis followed by its consumption and generation of hydrocarbons derivatives. The current efficiency was estimated considering the values of inorganic carbon (IC) reached after photoelectrochemical treatment, adapting equation previously established [35,36]:

$$CE(\%) = \frac{[(IC)_{\text{e}} - (IC)_{\text{p}}]}{8 I \Delta t} FV100 \quad (1)$$

Where $(IC)_0$ and $(IC)_t$ are the inorganic carbon (g L^{-1}) at times 0 and t , respectively, I is the current (A), F is the Faraday constant (26.8 Ah), V is the volume (L) and Δt is the time of treatment (h). Thus, the current efficiency for the process is only 34.9%. The results are similar to faradaic efficiency (38%) observed for CO_2 conversion on electrodeposited cuprous oxide electrodes, but these experiments were conducted at -1.1 vs SCE [37], which is much higher than in photoelectrochemical reduction.

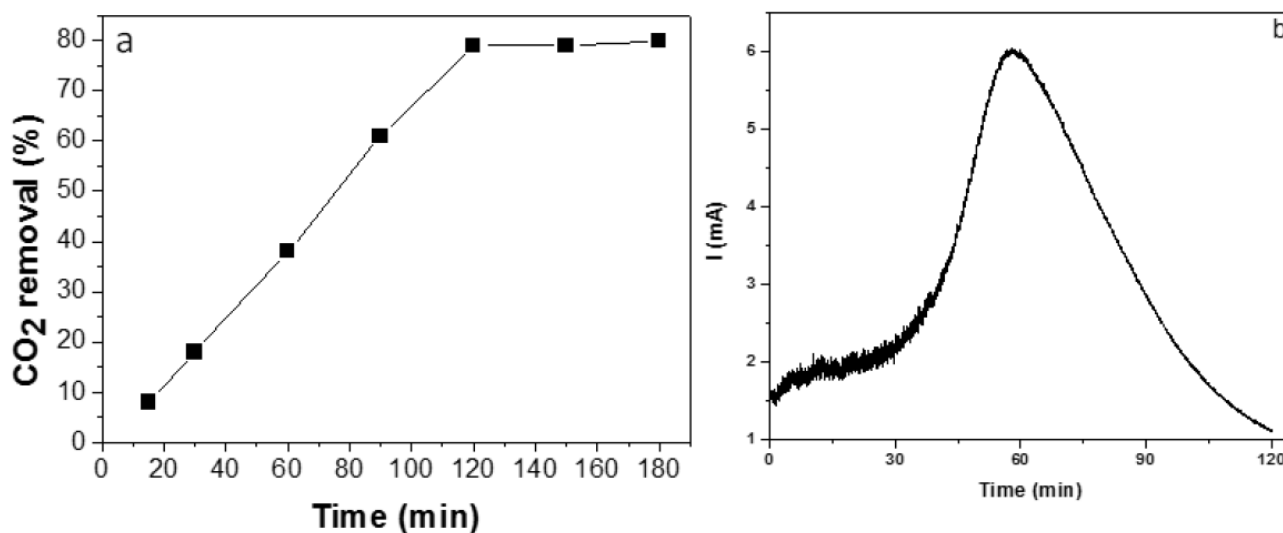


Figure 3. (a) Photoelectrochemical CO_2 reduction on the Cu/Cu₂O electrode in 0.3 mol L^{-1} sodium carbonate, pH 9. (b) current vs photoelectrolysis time of CO_2 curves.

Taking into consideration that the CO_2 reduction could be accompanied by formation of different hydrocarbons products via addition of electrons and protons or by deprotonation of intermediates [10], further studies were conducted measuring the methanol and ethanol formation during the process. For these parameters such as: applied potential, pH and supporting electrolyte type were evaluated.

3.2.1 Effect of supporting electrolyte

Figure 4 exhibits the CO_2 reduction (Figure a) carried out for photoelectrolysis conducted at Cu/Cu₂O electrode at bias potential of $+0.20 \text{ V}$ and UV-Vis irradiation in $0.1 \text{ mol L}^{-1} \text{ Na}_2\text{CO}_3$, $0.1 \text{ mol L}^{-1} \text{ NaHCO}_3$, and $0.1 \text{ mol L}^{-1} \text{ Na}_2\text{CO}_3/\text{NaHCO}_3$ pH 9. In each case was compared the percentage of CO_2 reduction (Figure 4a) and the concomitant formation of methanol and ethanol (Figure 4b).

The percentage of CO_2 reduction obtained after 2 h of photoelectrochemistry reaches values around 77%, regardless of the supporting electrolyte, but the products differ drastically in each electrolyte. There is formation of 80 ppm of methanol in $0.1 \text{ mol L}^{-1} \text{ Na}_2\text{CO}_3/\text{NaHCO}_3$, however, these values reached only 10 ppm in Na_2CO_3 and it is almost neglected in NaHCO_3 .

The mechanism of products formation by means of CO₂ photoelectroreduction is not still completely understood, but it is known that the electrochemical potentials for the reduction of CO₂ to CO₂^{•-} is around -1.9 V vs NHE, but the thermodynamic barriers can be reduced by photons energy [16]. Thus, it is possible to reduce CO₂ to CO₂^{•-} indirectly by photoelectrocatalytic process involving Cu (I) / Cu (II) oxidation at a potential so low as +0.20V vs Ag/AgCl. The preponderant synthesis of methanol is [37]:

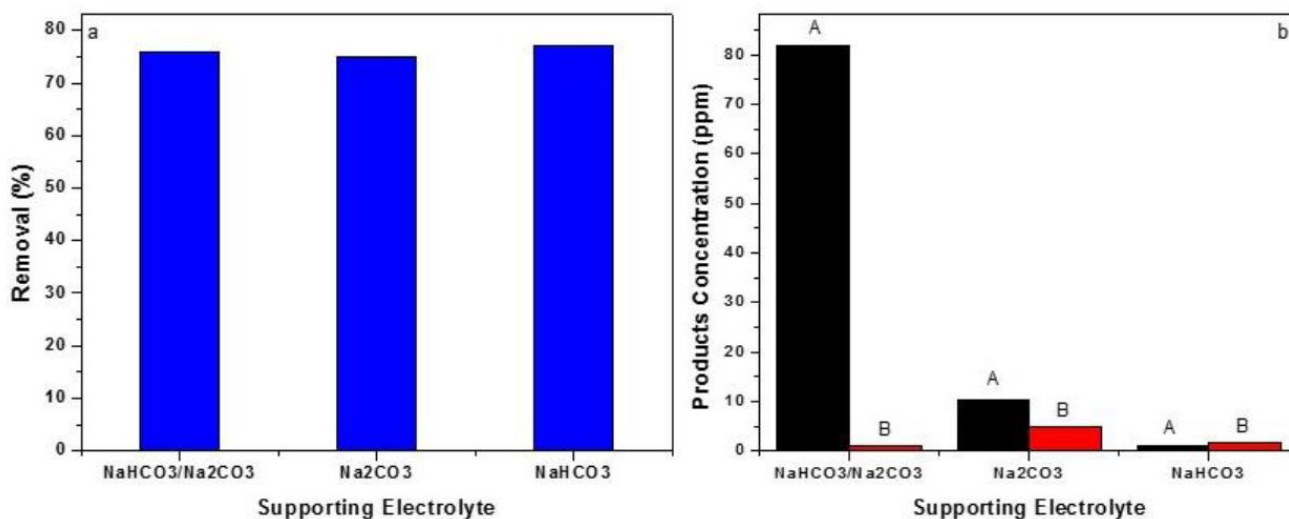


Figure 4. (a) Percentage of CO₂ reduction in 0.1 mol L⁻¹ NaHCO₃/Na₂CO₃, 0.1 mol L⁻¹ Na₂CO₃, and 0.1 mol L⁻¹ NaHCO₃ pH 9, after 2 h of photoelectrolysis under +0.2 V potential and UV radiation. (b) Concentration of methanol (A) and ethanol (B) generated after 2 h.



The synthesis of hydrocarbons from CO₂ is a complex multistep reaction with adsorbed intermediates and hydrogenation reaction that interferes drastically in pathway to obtain predict chemicals [16,17]. Thus, the main reduction products are influenced by adsorption of CO₂ and or CO₂^{•-} at Cu (I) site, and the thermodynamic barrier involving hydrogenation reaction as concurrent reaction.

Several electrochemical and photoelectrochemical routes [37] have proposed that the increase in methanol yields is associated with cuprous oxide film where the Cu (I) species play a key role in reducing CO₂. The Cu (I) sites were believed to stabilize reaction intermediates important to generated methanol. The results present in this paper suggest that the stability of the oxides Cu₂O in Na₂CO₃/NaHCO₃ buffer solution is satisfactory and hydrogenation of an adsorbed intermediate such as CO may be hydrogenated via proton transfer to form methanol. Thus the Na₂CO₃/NaHCO₃ buffer solution at moderately alkaline solutions promoted moderate corrosion of copper anodes, involving the formation of hydroxides soluble specie at positive potentials [38].

In order to test the leaching of copper from the electrode during a photoelectrocatalytic reduction of CO₂ carried out at Cu/Cu₂O electrode during 2 h in 0.1 mol L⁻¹ Na₂CO₃/NaHCO₃ buffer solution, potential of + 0.2 V and UV-Vis irradiation, the copper was analyzed by anodic stripping

voltammetry. The results indicated that no one of the solutions after photoelectrochemical reduction show the presence of copper ions, that indicates the copper oxide was not dissolved in the solution.

Thus, our findings confirm that Cu (I) / Cu (II) probably occurs via photons incidence, but the electrons on the conduction band (e^-) are trapped by CO_2 and Cu (II) species generated on photocathode, that is reduced to the Cu_2O . Therefore, there is no free copper ion in the solution. In the $\text{Na}_2\text{CO}_3/\text{NaHCO}_3$ buffer solution case, it is easy to maintain the same composition and pH, due to the carbonic acid-bicarbonate equilibrium. By using carbonate and bicarbonate, the local concentration of hydroxide ions at the interfacial region can be important in the hydration process of Cu_2O . These could be affecting the adsorption of CO_2 or the protonation of intermediates produced on copper oxide surface. Thus, the $0.1 \text{ mol L}^{-1} \text{ Na}_2\text{CO}_3/\text{NaHCO}_3$ buffer solution was selected as the best condition for further studies.

3.2.3 Effect of applied potential

Copper surfaces are free of oxides at potentials more negative than -0.50V vs Ag/AgCl in NaOH solution (0.1 to 1.0 mol L^{-1}), wherever the oxidation of Cu (I) to Cu (II) usually occurs around 0 V vs Ag/AgCl [39]. The photocatalytic reduction of CO_2 under UV light is well known in literature [40]. In order to understand the effect of applied potential on CO_2 reduction at Cu/ Cu_2O electrode under UV-Vis irradiation photoelectrolysis were carried out for 100 ppm of CO_2 solubilized in $0.1 \text{ mol L}^{-1} \text{ Na}_2\text{CO}_3/\text{NaHCO}_3$ buffer solution, pH 9.0, at potentials ranging from -0.4 V to $+0.2 \text{ V}$. The percentage of CO_2 reduction and the concomitant formation of methanol and ethanol are shown in Figure 5a and Figure 5b, respectively.

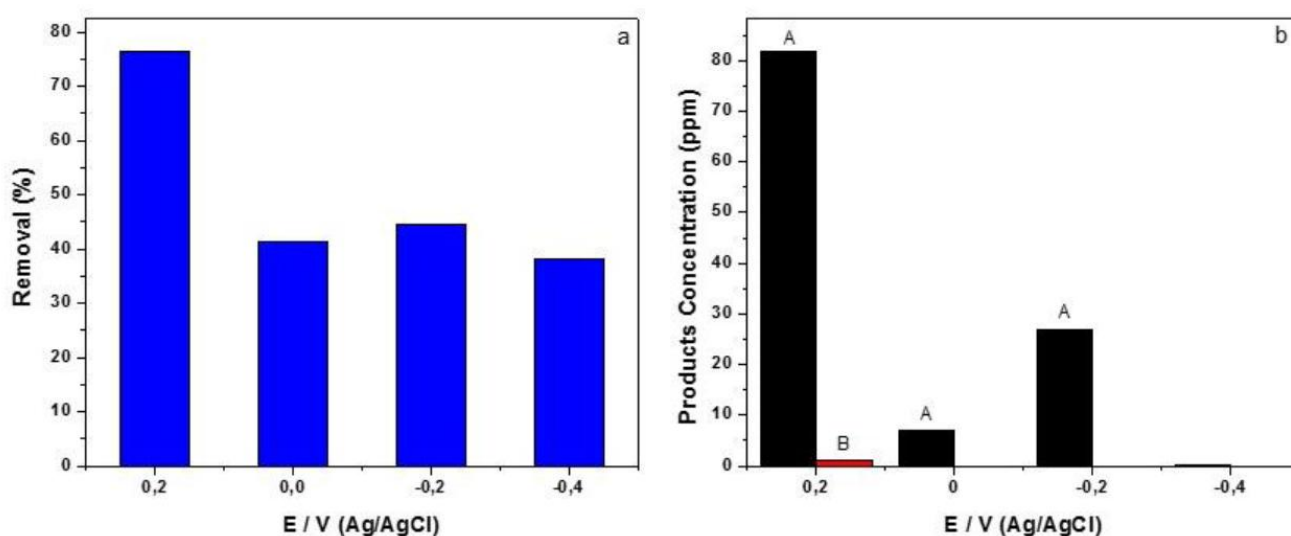


Figure 5. (a) Removal percentage of CO_2 after 2 h of photoelectrolysis in 0.1 mol L^{-1} sodium carbonate/bicarbonate buffer solution pH 9 at potentials ranging from -0.4 V to $+0.2 \text{ V}$ vs Ag/AgCl under UV-Vis irradiation. (b) Amount of methanol (A) and ethanol (B) formed after 2 h of photoelectrolysis.

The removal of CO₂ reaches only 40 % for applied potential inferior to 0 V and it is 75 % at bias potential of +0.2 V (Figure 5a). Concomitantly, the methanol production at -0.4 V is negligible as well as the ethanol formation, but it rises as the potential goes up to -0.2 V and is maxima at potential of 0.2 V (82 ppm), which corresponds to a yield of approximately 62 % of all CO₂ reduced. The high percentage of methanol generated at +0.2 V indicates better selectivity toward this product and confirms that CO₂ reduction occurs on the Cu/Cu₂O electrode using the redox cycle of Cu⁺/Cu⁺² system. At more negative potential ($E \geq -0.2$ V) the close proximity of the reduction potential H⁺/H₂O to H₂ may also occur as a concurrent reaction and the photoelectroreduction of carbon dioxide decreases [32]. These results confirm that the potential gradient only improves the scavenging of the electrons generated by UV-Vis radiation on the electrode surface. This potential is much slower than direct electrochemical reduction of CO₂ on metallic electrodes that usually requires a potential between -1.9 and -2.5 V vs NHE, depending on the solvent and electrolyte [16]. The lower potential required in photoelectrocatalytic process minimize the main competitive reactions involve hydrogen formation and the generation of a mixture products, such as CO, CH₄ and formic acid described in literature [32].

3.2.4 Effect of pH

In order to enhance methanol formation during CO₂ reduction, the pH influence was studied in 0.1 mol L⁻¹ sodium carbonate/bicarbonate buffer solution at pH 8 - 11, under applied potential of +0.2 V and UV- Vis irradiation. Figure 6 shows the influence of pH on CO₂ reduction (Figure 6a) and the concomitant formation of methanol and ethanol (Figure 6b) after 120 min of photoelectrochemical treatment. The results indicates that at pH 9 there is maximum CO₂ reduction (75%), but at pH 11 there is a clear CO₂ removal decays (36%), and the measured alcohol substances is virtually negligible at pH 11 (Figure 6b).

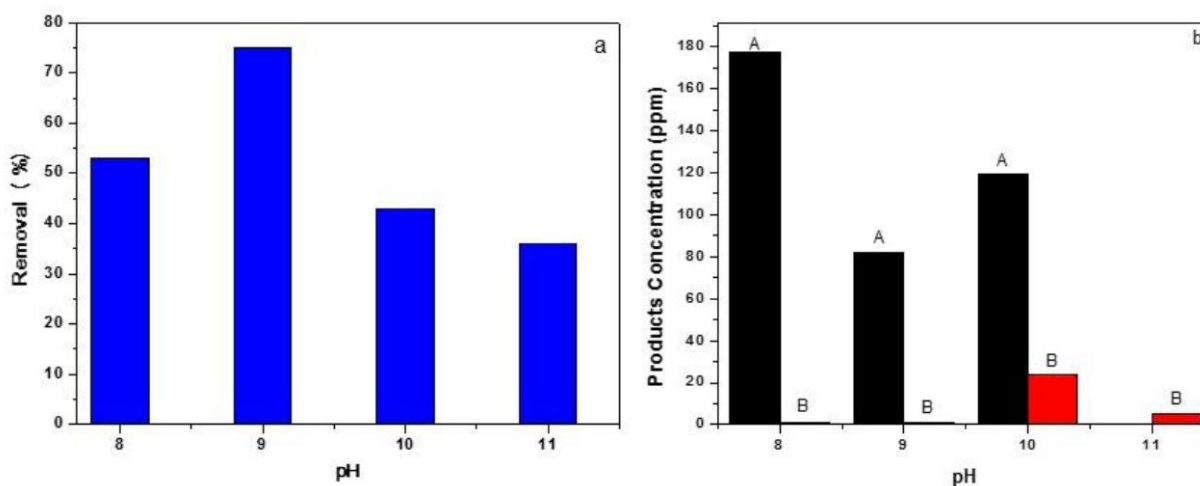


Figure 6. (a) Removal percentage of CO₂ after 2 h of photoelectrolysis at +0.2V in 0.1 mol L⁻¹ sodium carbonate/bicarbonate buffer solutions with pH ranging from 8 to 11 under UV-Vis light. (b) Quantification of the formed compounds methanol (A) and ethanol (B) after 2 h of photoelectrolysis.

Although CO₂ reduction in pH 8 reached only 54 % after 2 h of photoelectrolysis the methanol formation is 177 ppm achieving a corresponding to 97 % photoconversion of CO₂ / CH₃OH and demonstrating that the reaction is practically selective for this product in these conditions. It is interesting to observe that from the catalytic point of view, the selectivity of CO₂ reduction on Cu/Cu₂O photoelectrode might depend on pH, since the rate-determining step involves adsorption of CO₂ and/or intermediates that improves the transfer electrons and protonation reaction subsequently.

The influence of the pH can be explain with respect to species present in which case. According Zeebe and Wolf-Gladrow [41] in pH 8, the CO₂ dissolved is present as CO₂/HCO₃⁻, in pH 9 the CO₂ is almost equally divided between the HCO₃⁻ / CO₃²⁻ species and in pH 10 there are more CO₃²⁻ species than HCO₃⁻ species, and in pH 11 the predominance is almost totally of CO₃²⁻ species.

Thus, distribution of this species according with the pH of the supporting electrolyte can explain the difference between the percentage of the CO₂ reduced in each case, as well as, the concentration and the type of the alcohol formed. Previous studies [42,43] often stated that CO₂ is the reducible species to form methanol, while bicarbonate was reduced to form formate [38] and in HCO₃⁻ solution, methane is produced preferentially [10]. This is consistent with our result in terms of enhanced production of methanol in the Na₂CO₃/NaHCO₃ buffer solution as electrolyte starting at pH 8, since this electrolyte contains a relatively high concentration of CO₂.

The large number of mechanism proposed in the literature to the electrochemistry reduction, even as photocatalysis and photoelectrocatalysis reduction, of CO₂ lead us to believe that this subject has still not been elucidated [16]. But, seems that the key step in CO₂ reduction by photoelectrocatalysis is the Cu (I) that under light irradiation is oxidized by lacunes on conduction band and the electrons are directly transferred to CO₂ as indicated by Ghadimkhani and coworkers [22]. This double pathway for injection of photoelectrons into CO₂ could contribute to the enhanced photoelectrochemical response and promotion of the high conversion to methanol.

4. CONCLUSION

The importance of Cu (I) in the photoelectrochemical reduction of CO₂ to CH₃OH is demonstrated at Cu/Cu₂O electrode. The reduction occurs preponderantly due electrons that are generated due photoactivation of electrode under UV- Vis irradiation. Concomitantly, the redox cycle of Cu⁺¹/Cu⁺² at +0.20 V vs Ag/AgCl are generated preferentially due lacunas that can oxidized the Cu⁺¹. The applied potential amplifies the electron/lacunas separation on the electrode and the process leads to 80% of CO₂ removal and predominant methanol formation. The reaction reached 97 % of CO₂ reduction after 2 h of photoelectrolysis conducted for dissolved carbon dioxide in Na₂CO₃/NaHCO₃ the 0.1 mol L⁻¹ pH 8, at +0.20 V vs Ag/AgCl.

Our findings indicate that the coupling of bias potential, UV-Vis irradiation and a semiconductor like Cu₂O could be a good strategy to obtain a more effective and economic method that converts carbon dioxide into added value products. Due to the complexity of the process, further studies are necessary to improve selectivity and electrode stability, with a view to improve future applications.

ACKNOWLEDGEMENTS

Financial support from the Brazilian funding agencies FAPESP (2008/10449-7 and 2012/02725-0), CAPES, and CNPq are gratefully acknowledged.

References

1. S. Qin, F. Xin, Y. Liu, X. Yin, W. Ma, *J. Colloid Interface Sci.*, 356 (2011) 257.
2. H. Slamet, W. Nasution, E. Purnama, K. Riyani, J. Gunlazuardi, *World Appl. Sci. J.*, 6 (2009) 112.
3. R. Aydin, F. Köleli, *J. Electroanal. Chem.*, 535 (2002) 107.
4. S. J. T. Hangx, *CATO Workpackage WP 4.1*, (2005) 1.
5. S. Ohya, S. Kaneco, H. Katsumata, T. Suzuki, K. Ohta, *Catal. Today*, 148 (2009) 329.
6. K. Gao, K. R. McKinley, *J. Appl. Phycology*, 6 (1994) 45.
7. D. R. Sauerbeck, *Nutr. Cycl. Agroecosyst.*, 60 (2001) 153.
8. M.M. Halmann, M. Steinberg, *Greenhouse gas carbon dioxide mitigation: science and technology*, Lewis Publishers, Boca Raton, Florida, 1999.
9. M. E. Galvez, P. G. Loutzenhiser, I. Hischier, A. Steinfeld, *Energy Fuels*, 22 (2008) 3544.
10. Y. Hori, A. Murata, R. Takahashi, *J. Chem. Soc. Faraday Trans. I*, 85 (1989) 2309.
11. H. Noda, S. Ikeda, A. Yamamoto, H. Einaga, K. Ito, *Bull. Chem. Soc. Jpn.*, 68 (1995) 1889.
12. M. Gattrell, N. Gupta, A. Co, *J. Electroanal. Chem.*, 594 (2006) 1.
13. Y. Hori (2008) In: Vayenas CG, White RE, Gamboa-Aldeco ME (eds) *Modern Aspects of Electrochemistry*, Springer, New York, 2008.
14. Y. Terunuma, A. Saitoh, Y. Momose, *J. Electroanal. Chem.*, 434 (1997) 69.
15. K. P. Kuhl, E. R. Cave, D. N. Abram, T. F. Jaramillo, *Energy Environ. Sci.*, 5 (2012) 7050.
16. M. Jitaru, *J. Univ. Chem. Tech. Metall.* 42 (2007) 333.
17. O. K. Varghese, M. Paulose, T. J. LaTempa, C. A. Grimes, *Nano Lett.*, 9 (2009) 731.
18. S. Sato, T. Arai, T. Morikawa, K. Uemura, T. M. Suzuki, H. Tanaka, T. Kajino, *J. Am. Chem. Soc.* 133 (2011) 15240.
19. S. C. Roy, O. K. Varghese, M. Paulose, C. A. Grimes, *ACS Nano*, 4 (2010) 1259.
20. A. L. Linsebigler, G. Lu, J. T. Yates, *Chem. Rev.*, 95 (1995) 735.
21. H.O. Finklea (Ed.), *Semiconductor Electrodes*, Elsevier, New York, 1988.
22. G. Ghadimkhani, N. R. Tacconi, W. Chanmanee, C. Janaky, K. Rajeshwar, *Chem. Commun.*, 49 (2013) 1297.
23. M. V. B. Zanoni, J. J. Sene, M. A. Anderson, *J. Photochem. Photobiol. A: Chem.*, 157 (2003) 55.
24. B. A. Blajeni, M. Halmann, J. Manassen, *Sol. Energy Mater.*, 8 (1983) 425.
25. B. R. Eggins, J. T. R. Irvine, E. P. Murphy, J. Grimshaw, *J. Chem. Soc. Chem. Commun.*, 16 (1988) 1123.
26. T. Inoue, A. Fujishima, S. Konishi, K. Honda, *Nature*, 277 (1979) 637.
27. M. Halmann, *Nature*, 275 (1978) 115.
28. T. D. Golden, M. G. Shumsky, Y. Zhou, R. A. Vanderwerf, R. A. V. Leeuwen, J. A. Switzer, *Chem. Mater.*, 8 (1996) 2499.
29. F. M. M. Paschoal, L. Nuñez, M. R. V. Lanza, M. V. B. Zanoni, *J. Adv. Oxid. Technol.*, (2013) 63.
30. K. L. Sower, A. Fillinger, *J. Electrochem. Soc.*, 156 (2009) F80.
31. Sawyer, D. T.; Heineman, W. R.; Beebe, J. M. *Chemistry experiments for instrumental methods*. New York: John Wiley & Sons, 1984.
32. P. E. Jongh, D. Vanmaekelbergh, J. J. Kelly, *J. Electrochem. Soc.*, 147 (2000) 486.
33. Slamet, H. W. Nasution, E. Purnama, S. Kosela, J. Gunlazuardi, *Catal. Commun.*, 6 (2005) 313.
34. T. Kakumoto, *Energy Convers. Mgmt.*, 36 (1995) 661.
35. D. Rajkumar, J.G. Kim, K. Palanivelu, *Chem. Eng. Technol.*, 28 (2005) 98.
36. T.T. Guaraldo, S.H. Pulcinelli, M.V.B. Zanoni, *J. Photochem. Photobiol. A*, 217 (2011) 259.

37. M. Le, M. Ren, Z. Zhang, P.T. Sprunger, K. L. Kurtz, J. C. Flake, *J. Electrochem. Soc.* 158 (2011) E45.
38. P. Dubé, G. M. Brisard, *J. Electroanal. Chem.*, 582 (2005) 230.
39. T.R.L. Paixão, E. A. Ponzio, R. M. Torresi, M. Bertotti, *J. Braz. Chem. Soc.*, 37 (2006) 374.
40. M. Azuma, K. Hashimoto, M. Hiramoto, M. Watanabe, T. Sakata, *J. Electrochem. Soc.*, 137 (1990) 1772.
41. R. E. Zeebe, D. Wolf-Gladrow, *CO₂ in seawater: equilibrium, kinetics and isotopes*, Amsterdam: Elsevier Science, 2001.
42. T.E. Teeter, P. Van Rysselberghe, *J. Chem. Phys.* 22 (1954) 759.
43. R. Kortlever, K. H. Tan, Y. Kwon, M. T. Koper, *J. Solid State Electrochem.*, 17 (2013) 1843.

© 2014 The Authors. Published by ESG (www.electrochemsci.org). This article is an open access article distributed under the terms and conditions of the Creative Commons Attribution license (<http://creativecommons.org/licenses/by/4.0/>).